DOI 10.5162/Ultrasonic2025/P1.41

Characterizing Elasticity of NiTi Epitaxial Film in Austenitic Phase by Transient Grating Spectroscopy

David Mareš[1], *Kristýna Repček*[2], *Tomáš Grabec*[1], *Jakub Kušnír*[2], *Pavla Stoklasová*[1], *Petr Sedlák*[1], *and Hanuš Seiner*[1]
[1]*Institute of Thermomechanics of the Czech Academy of Sciences, Prague, Czechia*
[2]*Faculty of Nuclear Sciences and Physical Engineering, Czech Technical University in Prague, Prague, Czechia*
david.mares@it.cas.cz

Abstract: We employ transient grating spectroscopy (TGS) with a 7 µm excitation wavelength to analyze anisotropic elasticity of a thin supported film. The high sensitivity of TGS enables detection of multiple surface acoustic modes—Rayleigh, Sezawa (both with strong out-of-plane displacement), and Love (with transverse horizontal displacement)—in a slow-on-fast system of a 3µm thick epitaxial NiTi shape-memory alloy film on MgO, investigated in the austenitic state at 120 °C. Extracting elastic constants from angular dispersions is solved via the Ritz–Rayleigh method, enabling analysis of the cubic elastic constants of the NiTi film and provides valuable insights into the film's properties.

Keywords: transient grating spectroscopy, guided waves, elastic anisotropy, inverse procedure, shape-memory alloy

Introduction-Motivation

Characterizing elasticty of anisotropic thin films with micrometer-scale thickness is challenging. The traditional contact quasi-static techniques of micro- and nanoindentation using Oliver-Pharr [1, 2] analysis provide only limited information on the directional dependence of the elastic response. For this reason, a wide range of laser-ultrasonic approaches have been developed as alternatives, including picosecond ultrasonics, resonant ultrasound spectroscopy, surface-wave spectroscopy, and Brillouin spectroscopy. However, these methods provide only limited information about the elasticity and are often experimentally complex and time-consuming.

We employ transient grating spectroscopy (TGS) [3, 4], a laser-based optical method that relies on interference to achieve high sensitivity and strong k-vector selectivity both in the generation and detection of surface-guided acoustic waves. This approach enables precise measurements of surface acoustic waves (SAWs) at micrometer wavelengths, facilitating the determination of the angular dispersion of wave velocities.

Subsequently, a specifically designed minimization-based inverse procedure, combined with a Ritz-Rayleigh numerical model for elastodynamic properties of layered systems, allows for the precise determination of the elastic constants [5, 6, 7].

This allows us to study wave behavior in anisotropic films grown on anisotropic substrates [6], making it highly useful for non-destructive evaluation of epitaxial films. However, evaluating such layered systems is challenging. In addition to the well-known Rayleigh and Sezawa surface acoustic waves, which exhibit considerable out-of-plane motion, this is also sensitive to detect Love waves and their directional dispersion. Extensive experimental output also makes the inverse problem—extracting elastic constants from measured wave velocities—more complex. The analysis must account for how multiple propagation modes propagate in different directions, often intersecting with each other, and whose intersection points are linked to the very elastic constants being determined.

Methods - experimental setup

Transient grating spectroscopy (TGS), also referred to as impulse stimulated thermal scattering (ISTS) [8], is a laser-ultrasonic method designed for non-contact, non-destructive probing of acoustic properties in solids.It can, however, also be employed for the investigation of thermal properties [9]. The technique combines optical excitation of surface acoustic waves (SAWs) with their optical detection through light diffraction and consequent interference. Such optical heterodyne (interference) detection was first proposed by Maznev et al. [3]. In the present work, we employed the modified optical setup depicted in Figure 1, utilizing the differential heterodyne technique introduced by Verstraeten et al. [8].

In this work, we used TGS setup similar to that in Ref. [4]: SAWs are generated by a Nd:YAG pump laser (1064 nm, 0.55 ns, 200 µJ, 1 kHz) and detected by

DOI 10.5162/Ultrasonic2025/P1.41

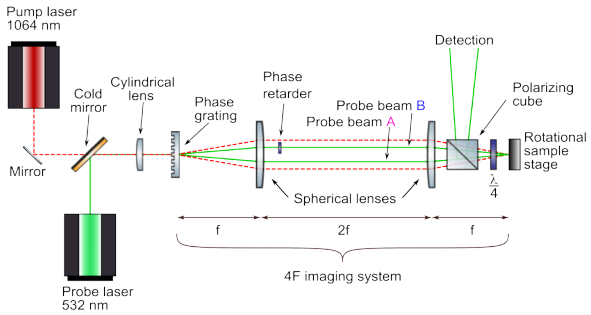

Fig. 1: The optical setup of the TGS method.

a continuous-wave probe laser at 532 nm (80 mW). A transmission grating splits both pump and probe laser beams into their ± 1 diffraction orders, while higher orders are blocked. The first-order beams are projected onto the sample surface using a 4F imaging system, where they interfere to form a periodic intensity pattern. The fringe spacing, and thus the acoustic wavelength, is determined by the incidence angle of the beams and can be easily adjusted by replacing the grating. Each interference fringe acts as a line-like thermoelastic source, launching SAWs with a well-defined wave vector perpendicular to the excitation fringes. The use of a cylindrical lens elongates the excitation pattern, further amplifying the excited k-vector. Because the laser energy is harmonically distributed across a large area, surface damage is avoided, enabling repeated non-destructive measurements, which are ideal for angular-dispersion characterization.

The probe beams, also diffracted into ± 1 orders and recombined on the surface, are sensitive to the transient grating created by the propagating SAWs. The optical setup forms the Littrow configuration, where each probe beam diffracts in the reflection direction of the other, enabling heterodyne detection. Detection is therefore carried out in the phase grating mode by carefully tuning the phase difference between the interfered beams (heterodyne phase $\approx \pi/2$), which maximizes sensitivity to out-of-plane displacements. The signal-to-noise ratio and sensitivity are further enhanced by measuring the intensity using Si photodiodes in a differential setup. Furthermore, since the pump and probe patterns overlap, near-field detection enables the detection of various higher-order modes, including those with very low out-of-plane components. The modulated probe signal, proportional to the instantaneous surface displacement, is captured by an oscilloscope. Averaging thousands of time traces enhances resolution and reduces noise. To determine SAW velocities and angular dispersion, time profiles were obtained for each measured direction. The frequency spectrum of the signal reveals the SAW frequency, from which its velocity is calculated as $v = \lambda f$, with λ determined by the interference pattern.

The angular dispersion of the wave velocities was obtained by rotating the sample with respect to the interference pattern. We carried out a 45° angular scan (with a step of 1°). To measure wave velocities at elevated temperature, a Peltier module was used to achieve a controlled temperature of 120 °C, ensuring that the NiTi film is in its single-crystalline austenite phase.

Methods - numerical

To determine the elastic constants from the measured angular-dependent velocities of guided waves, we have developed an inverse procedure that compares measured dispersive characteristics with theoretical predictions and iteratively adjusts material parameters until good agreement is obtained. For the forward problem, where material parameters are known and velocities are calculated, we use the Ritz-Rayleigh approach – a variational scheme of discretized functional space that converts the continuous wave equation into a discrete eigenvalue problem [5, 10]. This approach enables the calculation of guided-wave modes in generally anisotropic and layered media. However, to determine the elastic constants of a sample, the inverse method must be applied, whereby elasticity is calculated from measured wave velocities. An optimization algorithm is used to update the elastic constants until the misfit function iteratively

$$F(\mathbf{c}) \;=\; \sum_{p} \left(v_p^{\mathrm{cal}}(\mathbf{c_i}) - v_p^{\mathrm{exp}}\right)^2 \;\rightarrow\; \min_{\mathbf{c}}\,. \qquad (1)$$

reaches a minimum. At each iteration, the forward problem is recalculated, producing new dispersion curves that are compared to the experiments. Convergence indicates that the estimated constants reproduce the observed guided-wave dispersion with sufficient accuracy.

Study case

The sample used in this study was a thin film of NiTi shape memory alloy. The film was epitaxially grown [11] by DC magnetron sputtering on a single-crystalline MgO(100) substrate. To reduce epitaxial stress, buffer layers of vanadium and chromium were used, with a combined thickness of 50 nm. The epitaxial relationship between the NiTi austenite (B2 structure) and the MgO substrate was MgO(100)[001] ∥ V/Cr(100)[011] ∥ NiTi B2(100)[011]. This indicates that the austenite unit cell is rotated by 45° around the substrate normal relative to the film, such that of MgO aligns with of the austenite (as shown in Fig. 2a). The film thickness was measured by scanning

DOI 10.5162/Ultrasonic2025/P1.41

electron microscopy on a cross-section prepared by focused ion beam milling using a FEI Helios NanoLab 600i, the determined value being 3060 nm (Figure 2b).

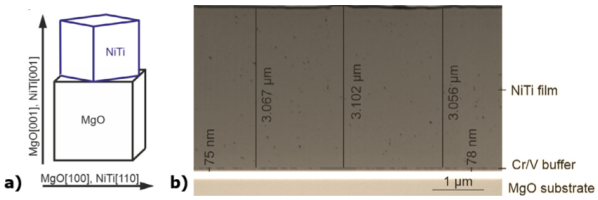

Fig. 2: a) Schematic showing B2 austenite unit-cell orientations of the film with respect to the substrate, b) cross-sectional SEM thickness measurement of the supported 3 µm thick NiTi layer on MgO substrate.

Results and Discussion

In this study, the acoustic wavelength of 7 µm was employed to probe the 3 µm NiTi film. This wavelength was chosen to achieve a balance between the surface confinement and the frequency range of the resulting acoustic signals. Since the acoustic energy of an SAW decays exponentially with depth, over a distance comparable to its wavelength, the 7 µm excitation ensures that a significant portion of the elastic field interacts with the film. Although shorter wavelengths would confine the wave more strictly within the film, they would require finer phase-grating periods, more demanding optical alignment, and higher detector resolution and frequency range. The selected wavelength thus represents an optimized compromise between the sensitivity of the film, the penetration depth, and the experimental practicality.

The TGS velocity map shown in Figure 3a revealed multiple guided modes. Modes were identified through signal strength, angular distribution, and the Ritz-Rayleigh inverse procedure, beginning with estimated elastic constants and the strongest signal corresponding to the Rayleigh-type surface wave. The angular dispersion shows a discontinuity near the middle of the measured angular dispersion. This is caused by a crossing with a Love-type wave with dominantly transverse horizontal polarization. The coupling of this Love-type mode with the Rayleigh-type mode results in a range of measured angles, where both modes are identifiable in the measured spectra. Two peaks corresponding to faster waves, observable across all angles, were identified as Sezawa-type modes. In non-principal crystallographic directions, another Love-type mode was detected via coupling-induced out-of-plane displacement.

NiTi austenite exhibits cubic symmetry, the elasticity of which can be described by three independent constants [12]. However, to allow for an effect of the epitaxial strain, tetragonal symmetry (with six independent elastic constants) was considered for the NiTi film. After the step-by-step identification of the experimentally observed wave modes in the measured angular scan, all six constants were determined. These constants exhibit cubic symmetry, proving that epitaxial strain is negligible and that three constants were sufficient to describe the measured angular dispersion (see the comparison of the experiment and calculation in Figure 3). The resulting elasticity was $c_{11} = 184.7 \pm 1.2$ GPa, $c_{12} = 149.7 \pm 1.3$ GPa, and $c_{44} = 33.19 \pm 0.04$ GPa.

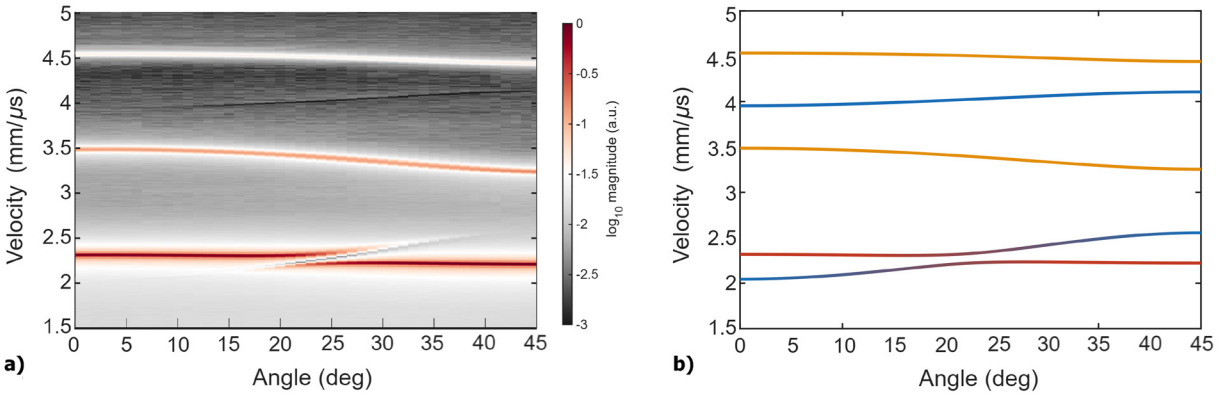

Fig. 3: Velocity maps of the epitaxial NiTi sample at 120 °C (i.e., in austenite) obtained by the angular TGS scan (a) and calculated with the Ritz–Rayleigh forward method with the determined elastic constants (b). The starting point of 0° corresponds to [001] direction of the MgO substrate. Note that the experimental map (a) is color-coded with a logarithmic scale of the signal magnitude. The modes in the calculated map (b) are color-coded as follows: Love-type wave modes are shown in blue, the Rayleigh-type mode in red, and Sezawa-type modes in orange.

Conclusion

In this work, we demonstrated the suitability of TGS for characterizing the elasticity of anisotropic micrometer-thin films on a substrate. We report TGS measurements of guided ultrasonic waves in epitaxially grown 3 µm NiTi thin film on MgO substrate and investigate the single-crystalline austenite phase at elevated temperature. The high sensitivity of TGS to surface-displacement dynamics allowed detection of Rayleigh, multiple Sezawa, and Love-type modes, providing sufficient information to characterize the elastic anisotropy of the film. We further show that the Ritz–Rayleigh numerical approach for guided waves enables solving the multimode inverse problem by single minimization, allowing to assess the elastic constants of the film. The resulting elasticity showed that at 120°C the single-crystalline austenite film remains elastically cubic.

Acknowledgment

This work was financially supported by the Czech Science Foundation [Project No. 22-13462S], Operational Program Johannes Amos Comenius of the Ministry of Education, Youth and Sport of the Czech Republic, within the frame of project Ferroic Multifunctionalities (FerrMion) [Project No.CZ.02.01.01/00/22_008/0004591], co-funded by the European Union and by the Grant Agency of the Czech Technical University [No. SGS25/168/OHK4/3T/14].

References

[1] S. Moyne et al. "Analysis of the thermomechanical behavior of Ti–Ni shape memory alloy thin films by bulging and nanoindentation procedures". In: *Materials Science and Engineering: A* 273-275 (1999), pp. 727–732. ISSN: 0921-5093. DOI: 10.1016/S0921-5093(99)00405-0.

[2] P. D. Tall et al. "Nanoindentation of Ni–Ti Thin Films". In: *Materials and Manufacturing Processes* 22.2 (2007), pp. 175–179. DOI: 10.1080/10426910601062222.

[3] A. A. Maznev, K. A. Nelson, and J. A. Rogers. "Optical heterodyne detection of laser-induced gratings". In: *Opt. Lett.* 23.16 (1998), pp. 1319–1321. DOI: 10.1364/OL.23.001319.

[4] P. Stoklasová et al. "Laser-Ultrasonic Characterization of Strongly Anisotropic Materials by Transient Grating Spectroscopy". In: *Experimental Mechanics* (2021). DOI: 10.1007/s11340-021-00698-6.

[5] P. Stoklasová et al. "Forward and inverse problems for surface acoustic waves in anisotropic media: a Ritz-Rayleigh method based approach". In: *Ultrasonics* 56 (2015), pp. 381–389. DOI: 10.1016/j.ultras.2014.09.004.

[6] T. Grabec et al. "Guided acoustic waves in thin epitaxial films: Experiment and inverse problem solution for NiTi". In: *Ultrasonics* 138 (2024). DOI: 10.1016/j.ultras.2023.107211.

[7] K. Repček et al. "Compliant Lattice Modulations Enable Anomalous Elasticity in Ni–Mn–Ga Martensite". In: *Advanced Materials* 36.39 (2024), p. 2406672. DOI: 10.1002/adma.202406672.

[8] B. Verstraeten et al. "Determination of thermoelastic material properties by differential heterodyne detection of impulsive stimulated thermal scattering". In: *Photoacoustics* 3.2 (2015), pp. 64–77. DOI: 10.1016/j.pacs.2015.05.001.

[9] J. Kušnír et al. "Apparent anisotropic thermal diffusivity measured in cubic single crystals by transient grating spectroscopy". In: *Journal of Applied Physics* 133.12 (2023), p. 125108. DOI: 10.1063/5.0136850.

[10] T. Grabec, P. Sedlák, and H. Seiner. "Application of the Ritz—Rayleigh method for Lamb waves in extremely anisotropic media". In: *Wave Motion* 96 (2020), p. 102567. DOI: 10.1016/j.wavemoti.2020.102567.

[11] K. Lünser et al. "How to grow single-crystalline and epitaxial NiTi films in (100)- and (111)-orientation". In: *Journal of Physics: Materials* 6.3 (May 2023), p. 035002. DOI: 10.1088/2515-7639/acd604.

[12] L. Bodnárová et al. "Elastic Constants of Single-Crystalline NiTi Studied by Resonant Ultrasound Spectroscopy". In: *Shap. Mem. Superelasticity* 11.2 (June 2025), pp. 230–238. ISSN: 2199-3858. DOI: 10.1007/s40830-025-00534-z.